HOW2POWER TODAY
Your Power Design Newsletter

Exclusive Technology Feature

ISSUE: June 2026

How Active EMI Filter ICs Reduce Common-Mode Emissions In Single- And Three-Phase Applications (Part 6): Unifying DM And CM AEF

by Timothy Hegarty, Texas Instruments, Phoenix, Ariz.

A high-density design of the front-end electromagnetic interference (EMI) filter is mandatory for ac-dc grid-tied power supplies used in size-constrained environments, such as rack-scale power shelves for data centers and on-board chargers (OBCs) for automotive. Benefiting from the miniaturization of toroidal-cored common-mode (CM) chokes, an active EMI filter (AEF) circuit to attenuate CM noise can substantially increase the power density of the EMI filter relative to a passive design while also reducing the weight and cost of the overall implementation.

Part 1 of this article series[1] provided an overview of AEF techniques to diminish the reliance on bulky passive filter components. Parts 2 and 3 discussed behavioral models to suitably characterize the impedance of ferrite[2] and nanocrystalline[3] chokes, respectively. Part 4 examined small-signal stability[4] by deriving loop-gain expressions for a feedback-type voltage-sense current-inject (FB-VSCI) AEF circuit, implemented using an IC. Part 5 delved into a multiple feedback technique[5] to improve immunity behavior below 150 kHz.

However, the resultant smaller CM chokes with AEF typically have a reduced leakage inductance, which compromises the achievable differential-mode (DM) attenuation. Leveraging an existing CM AEF implementation, this article, part 6 and the final installment of the series, pursues a unified AEF solution that offers active cancellation of both DM and CM emissions simultaneously. Experimental results from a two-stage LCLC single-phase EMI filter validate the proposed AEF circuit extension.

Active Filtering—Why Both DM And CM Attenuation Are Needed

Power electronics technologies play a crucial role in automotive, industrial and data center applications, enabling efficient power conversion. Such applications require kilowatt-scale, high-density power supplies, such as ac-dc boost power factor correction (PFC) rectifiers[6] that operate off the ac grid and meet stringent specifications for efficiency, cost, safety, reliability, volume, weight, line-frequency harmonics and, crucially, EMI.

The switching action of these power supplies is an inherent source of voltage-driven and current-driven noise sources, causing both DM and CM emissions that tend to propagate towards the ac grid or chassis ground (earth potential). Higher power levels and the increased number of fast-switching power devices in space-limited power conversion systems result in a more challenging electromagnetic environment, with additional EMI sources and victims present in end equipment such as server-rack power supplies, telecom rectifiers, and automotive OBCs.

Moreover, wide-bandgap (WBG) power semiconductors, such as gallium nitride (GaN) and silicon carbide (SiC), produce higher dv/dt and di/dt switching relative to silicon power devices. The inherently faster switching speed of WBG devices generally leads to increased conducted and radiated emissions. By necessity, regulatory bodies, such as CISPR[7] and IEC, specify limits for the total noise generated on each input power line of an ac supply. The total noise comprises DM and CM current components measured collectively at the line impedance stabilization network (LISN) when performing conducted emissions testing.

To achieve electromagnetic compatibility (EMC), there has been a significant increase in research focused on developing effective countermeasures to suppress conducted emissions. From this standpoint, the topic of active filtering[1-5, 8-11] attracts substantial attention in power-electronics-constrained applications, owing to the improvements in power density and cost relative to traditional passive filter networks. A cost-effective and high-density filter is a key challenge in switching regulator implementations and is essential to effectively package the complete solution within demanding chassis-enclosed form factors.

IEC 60990 specifies the maximum value of the protective conductor current to meet touch-current safety requirements.[12] As a result, EMI filters for grid-tied applications often have an upper bound for the total Y-capacitance value and thus require large-sized CM chokes to achieve a target corner frequency or filter attenuation. This can give rise to unsatisfactory passive filter designs with bulky CM chokes that impact the overall filter size.

Thankfully, high-density power-electronics applications can leverage commercially available CM AEF integrated circuits (ICs)[1] to reduce magnetic component and filter size by amplifying the effective value of Y-capacitance over a prescribed frequency range. This helps to comply with the applicable conducted emissions standards while increasing the volumetric and gravimetric power densities of the front-end EMI filter structure.

However, the resultant smaller CM chokes with fewer winding turns typically have a lower leakage inductance, which compromises the achievable DM attenuation.[8, 13] Adding a separate DM inductor or more X-capacitance to recoup the lost DM attenuation negates the weight and volume optimizations achieved thus far with the CM-only AEF. Active attenuation of the total noise signature, both DM and CM, becomes essential.[8-11]

Review Of AEF

Conducted Emissions Measurement

In the context of AEF, it is important to understand the DM and CM noise current paths. Depicted in Fig. 1 is the CISPR 32 setup[7] for measurement of conducted emissions from a chassis-enclosed ac-dc power supply. As shown, the CM currents flow in the same direction on the line and neutral power lines and then complete a return path through the ground plane.

Conversely, the DM currents flow in opposite directions on the power lines. Meanwhile, the CM disturbance voltage is the average of the noise voltages, V_1 and V_2, at the LISN, whereas the DM disturbance voltage is simply the difference between the two noise voltages.

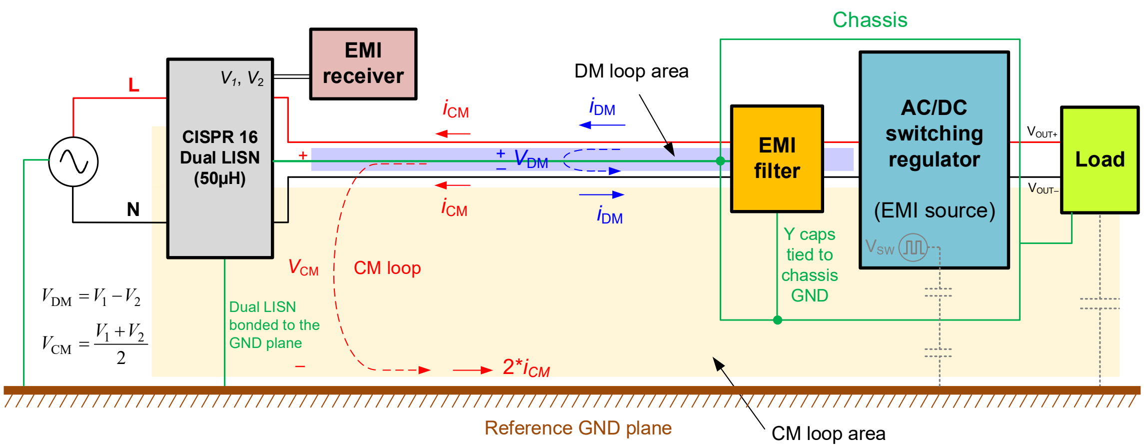

Fig. 1. CISPR 32 conducted emissions measurement setup with an ac-dc regulator, front-end EMI filter, dual LISN, and EMI receiver.

The equipment under test (EUT) mounts on a table 0.4 m above the measurement ground plane. The load may be tied to chassis for safety as shown or left floating. The dual LISN bonds to the ground plane, and an EMI receiver measures the two noise voltages over the prescribed frequency range.

Existing CM AEF Circuit—Structure

Shown in Fig. 2 are schematics for a two-stage LCLC passive-only filter design and an equivalent active filter implementation. The CM AEF solution uses a feedback voltage-sense, current-inject (FB-VSCI)[1] topology. The method provides a high level of integration by virtue of an IC approach and enables high density by using capacitors for sensing and injection, avoiding magnetic components. Placed between the CM chokes designated as L_{CM1} and L_{CM2} in Fig. 2, the AEF circuit provides a lower impedance shunt path for CM noise currents to flow to chassis ground.

The design targets a reduction of the filter volume yet maintains low values of the low-frequency earth leakage current using an active circuit that shapes the frequency response of the inject capacitor—effectively multiplying its value at high frequencies. In turn, this amplified inject capacitance over the required frequency range is the key to achieving lower CM choke inductances relative to the values of a passive filter with an equivalent attenuation profile.

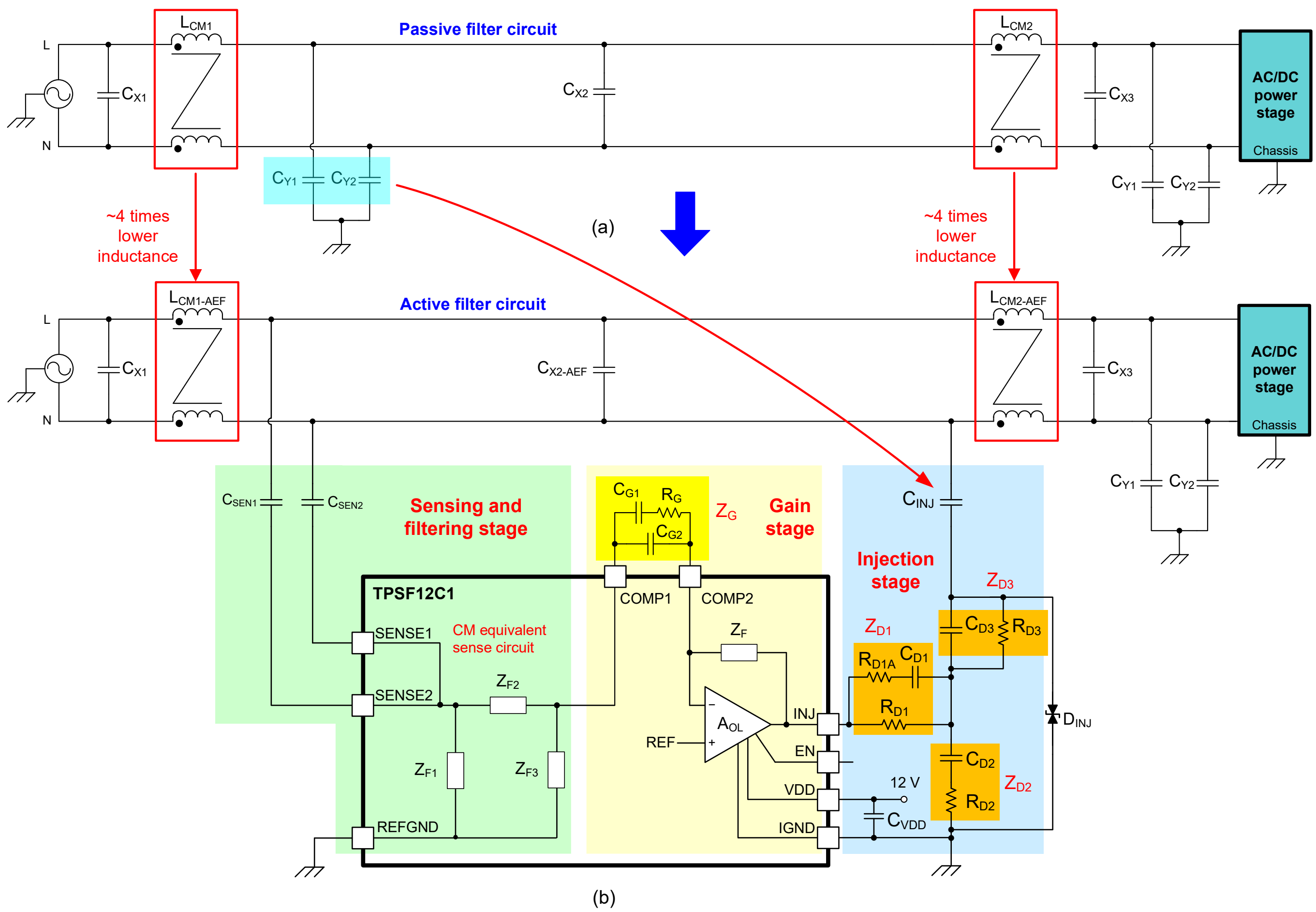

Fig. 2. Schematic of a two-stage, single-phase LCLC passive filter (a) that is replaced by a CM AEF circuit (b) with reduced CM-choke inductance values.

The CM AEF design in Fig. 2b leverages high-voltage Y-rated capacitors in combination with low-voltage active circuits within the IC for sensing and injection. The output of the power amplifier (at the INJ pin) injects the required noise-cancelling signal back into the power lines through a damping network and a Y-rated inject capacitor C_{INJ}.

X-capacitor C_{X2} positions between the CM chokes and effectively provides a low-impedance path between the power lines from a CM noise standpoint, up to low-MHz frequencies. This allows current injection directly onto one power line using just one inject capacitor. Inclusion of the damping network shapes the amplifier-output-to-inject-capacitor transfer function to stabilize the LC resonant behavior that occurs between the CM choke inductances and the inject capacitance.

Existing CM AEF Circuit—Impact On DM Attenuation

We define the impedance path in Fig. 2 through which the CM current flows to chassis ground as Z_{CM} and the impedance path through which the DM current flows from line to neutral as Z_{DM}. In the existing CM AEF topology, X capacitors act as Z_{DM} carrying the DM current, and Z_{Cinj}/G_{AEF} acts as Z_{CM} shunting the CM current to chassis ground.

However, an inherent limitation of this approach (and most CM AEF circuits) is that the CM chokes designated as $L_{CM1\text{-}AEF}$ and $L_{CM2\text{-}AEF}$ in the active circuit, while reduced in size relative to the chokes in a passive design, have lower leakage inductance[13] and thus provide less DM attenuation. In other words, achieving a reduction of CM noise, while often the main challenge, increases the DM noise signature. This necessitates the addition of a discrete, dedicated DM inductor or use of larger X-capacitors (that are typically limited in value by inrush, surge and power-factor considerations).

Ideally, the AEF circuit should simultaneously attenuate both the DM and CM noise components to obtain a reduction of the total noise on each power line, as measured by each LISN. Often, the end equipment produces substantial DM and CM interference and thus requires mitigation of both noise modes to meet the emissions limits prescribed by the applicable EMC standard.

Modifying The CM AEF Topology For Total Noise Attenuation

Extending The CM-Only AEF Circuit To Attenuate Both CM And DM Noise

Shown in Fig. 3 is the proposed AEF arrangement for total noise attenuation. We amalgamate two CM-only AEF circuits to provide dual AEF-cancellation loops of two symmetric circuits connected between the two power lines and chassis ground.

Represented in block diagram format in Fig. 3, the CM AEF IC is repurposed to sense the voltage disturbance on a power line with respect to chassis ground. Adhering to the current directions defined in Fig. 1, one AEF circuit ideally conducts a noise current of $I_L = I_{CM} + I_{DM}$ to chassis ground while the other conducts a noise current of $I_N = I_{CM} - I_{DM}$.

Using two AEF cancellation loops, the proposed configuration provides an alternate low-impedance path for DM noise current to flow between line and neutral where C_{X2} connects. The arrangement of each AEF IC is similar to that in Fig. 2 but with voltage sensing on just one power line using one sensing capacitor for each device. The SENSE2 pin of each IC ties to ground.

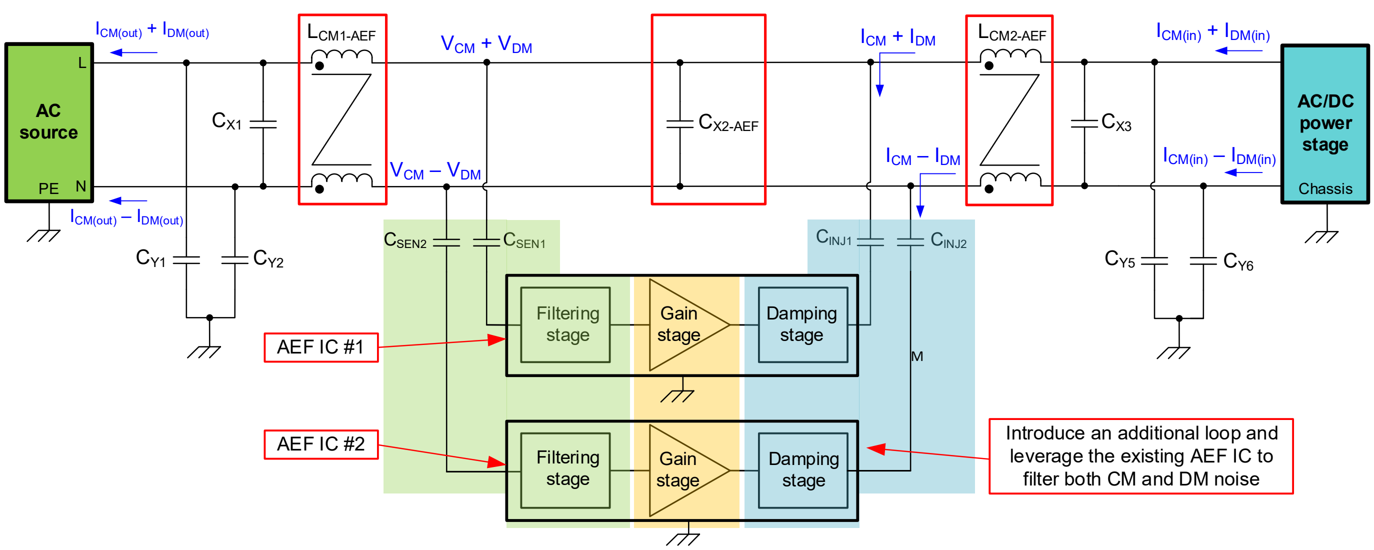

Fig. 3. Block diagram of a single-phase AEF circuit with DM and CM attenuation using two CM-only AEF circuits powered from a common bias supply referenced to chassis ground.

As before, the two AEF circuits contain the three main stages of AEF highlighted in Fig. 2 for sensing and filtering, gain, and injection. Voltage sensing and current injection methods again feature in this unified FB-

VSCI topology, thus preserving attributes of small size and lightweight. One bias supply referenced to chassis ground conveniently powers both ICs.

As depicted in Fig. 3, the two cancellation currents for DM are reverse in phase due to the polarity of the sensed voltage disturbance. One is positive cancellation current that flows from line to chassis, and the other is negative cancellation current from neutral to chassis. It can be treated as one DM cancellation current flowing from line to neutral, thus emulating the behavior of an X-capacitor that conducts DM noise.

The two loops provide a low effective impedance path for the DM current to flow, reducing the total DM impedance seen between line and neutral, thereby filtering the DM noise. Fig. 4 shows a schematic with two CM AEF ICs and the reduction in passive component values achievable by using the unified CM and DM AEF circuit.

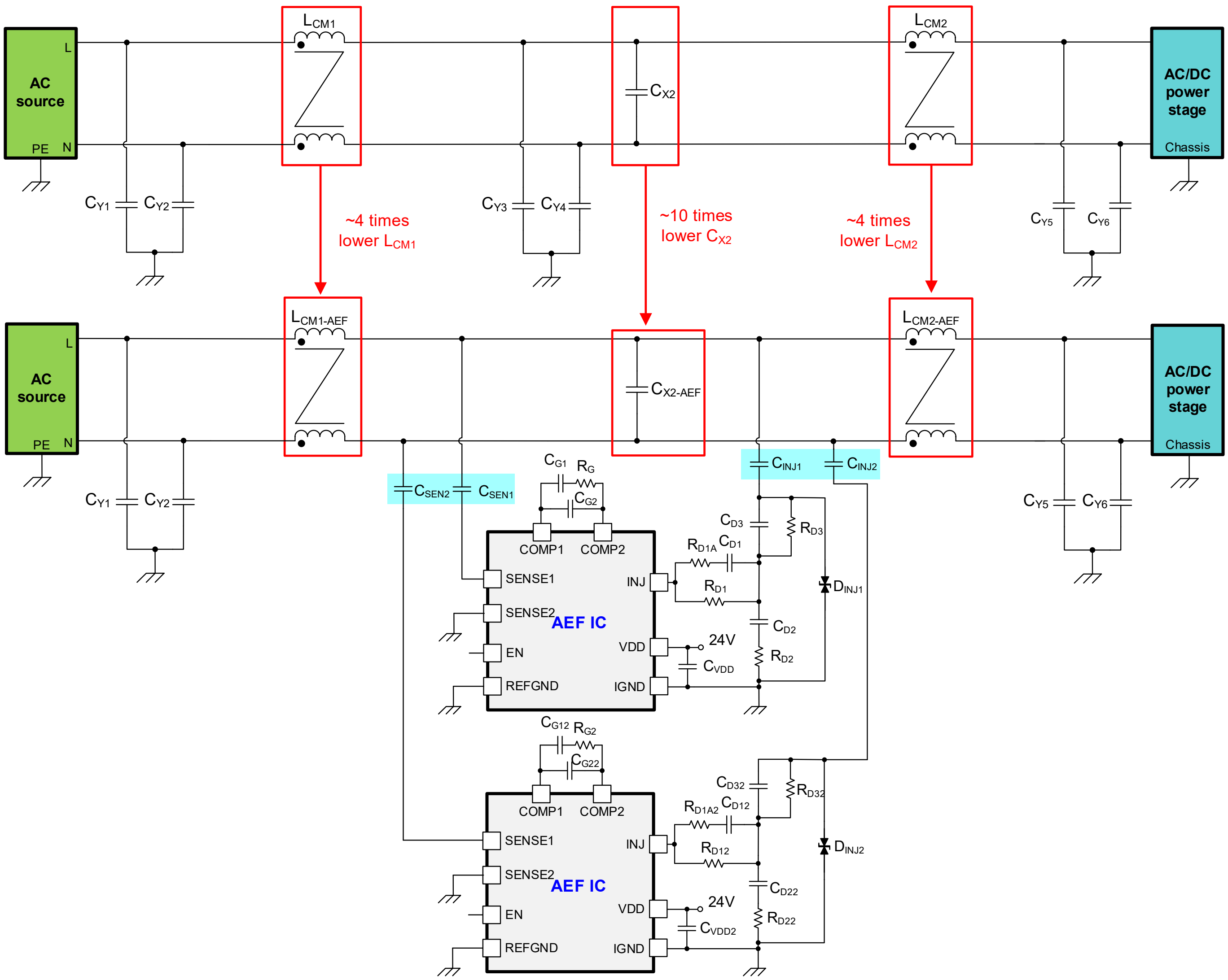

Fig. 4. Practical DM and CM attenuation using two CM-only AEF ICs.

DM And CM Impedances

The AEF amplifier in Fig. 2b establishes the closed-loop (CL) gain, which is the transfer function from the sensed and filtered CM disturbance at the COMP1 pin to the amplifier output at the INJ pin. This CL gain expresses as

$$A_{CL}(s) = -\frac{Z_F(s)}{Z_G(s)} \cdot \frac{1}{1 + \frac{\left(1 + Z_F(s)/Z_G(s)\right)}{A_{OL}(s)}} \quad (1)$$

where $A_{OL}(s)$ is the open-loop (OL) amplifier gain. The AEF gain $G_{AEF}(s)$ from LINE to INJ is then the total of the sensing gain $A_{SENSE}(s)$ from LINE to COMP1 and the CL gain $A_{CL}(s)$ from COMP1 to INJ. The AEF gain is important, as it determines the virtual impedance[1] reduction (or capacitance boosting effect) of the inject capacitor by the AEF circuit as:

$$Z_{AEF}(s) \approx \frac{Z_{Cinj}(s)}{1 - G_{AEF}(s)} \quad (2)$$

The AEF gain is then given by

$$G_{AEF}(s) = A_{SENSE}(s) A_{CL}(s) \quad (3)$$

The AEF noise sensing, processing and amplification circuits are generally optimized to produce high AEF gain, corresponding to maximum attenuation performance, for emissions in the EMI-measurement frequency band.

The proposed DM AEF impedance, effectively two CM AEF inject branches in series, is given by

$$Z_{DM}(s) = 2 Z_{AEF}(s) \quad (4)$$

while the CM AEF impedance, effectively two CM AEF inject branches in parallel, becomes

$$Z_{CM}(s) = \frac{Z_{AEF}(s)}{2} \quad (5)$$

Incorporating the second AEF loop provides the added benefit of reducing the effective CM impedance by a factor of two between line/neutral and chassis, thus improving the filter insertion loss for CM by 6 dB.

Analytical Results

Based on the expressions above and neglecting effects of equivalent series inductance (ESL) related to the X-capacitors, Fig. 5 shows a typical DM impedance profile for the existing passive filter and the proposed unified CM and DM AEF circuit with an X-capacitor C_{X2} of 220 nF.

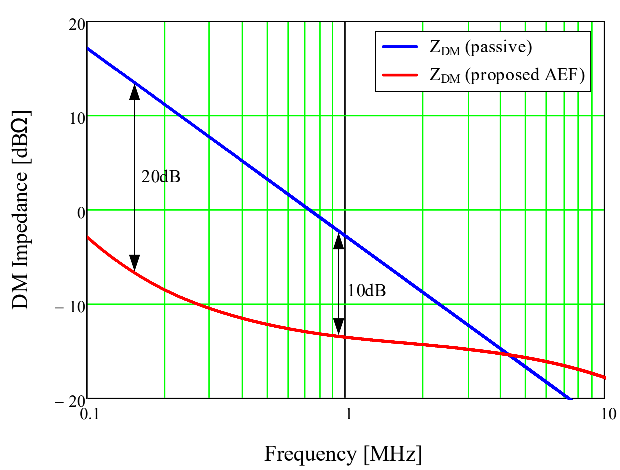

Fig. 5. DM impedance of the passive and proposed active filters with C_{X2} = 220 nF.

The AEF configuration provides approximately 20 dB and 10 dB lower impedance for DM disturbances at 150 kHz and 1 MHz, respectively. The absolute value of DM impedance reduces from 4.8 Ω to 0.5 Ω at 150 kHz. The passive and active impedance characteristics intersect at approximately 4 MHz due to limited gain-bandwidth performance of the AEF amplifier.

Experimental Results

Experimental Setup And Practical Results

Fig. 6 shows CISPR 32 measured EMI results using an experimental prototype circuit. The single-phase AEF evaluation board is rated at 10 Arms. The nanocrystalline-cored CM chokes from Würth Elektronik each have a rated CM inductance of 2 mH and DM (leakage) inductance of 1.6 µH. The Y-capacitors connected from the power lines to chassis ground at the grid and regulator sides of the filter are each set at 2.2 nF, and the Y-rated inject capacitors, C_{INJ1} and C_{INJ2} in Fig. 4, are both 10 nF.

The emissions result in Fig. 6 shows similar DM attenuation performance with X-capacitance, designated as C_{X2} in Fig. 4, of 2.2 µF (passive only) and $C_{X2\text{-}AEF}$ of 220 nF (unified AEF), giving an increased DM attenuation of 20 dB and aligning with the analytical result of Fig. 5. This demonstrates the virtual impedance reduction (capacitance boosting or amplifying effect) of DM AEF, akin to the Y-capacitance boosting effect associated with CM AEF.

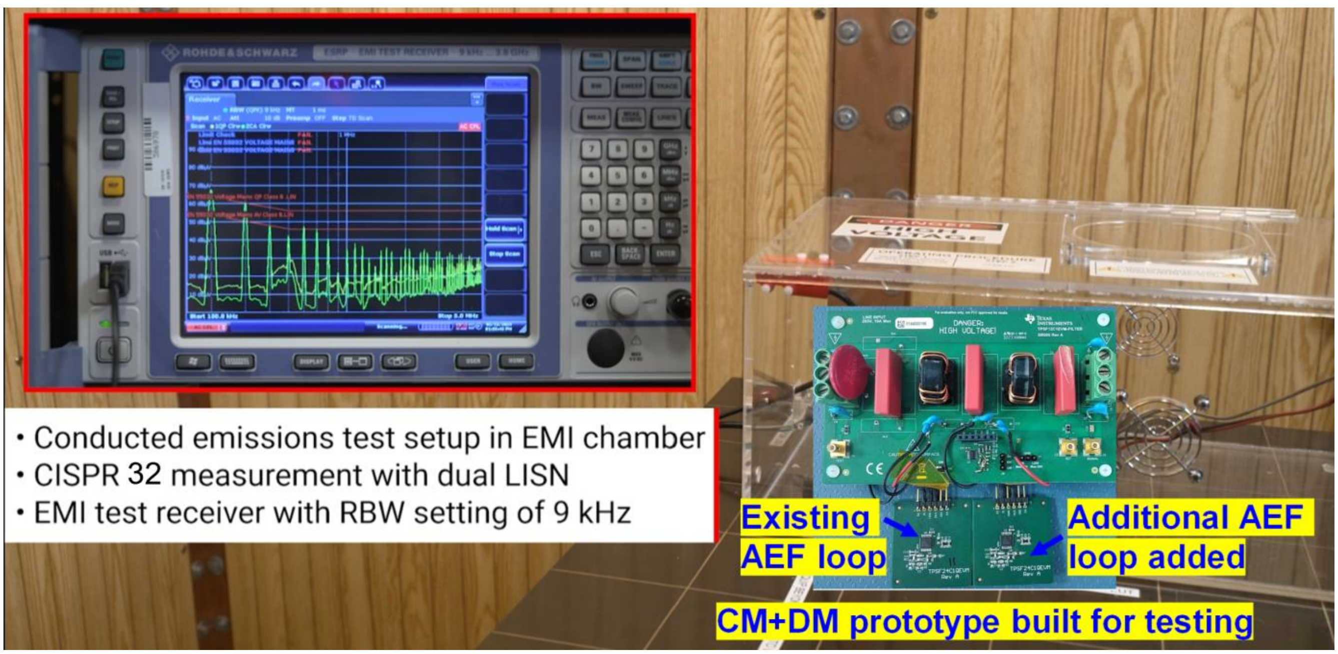

Fig. 6. Experimental measurements with the unified DM and CM AEF setup.

With a switching frequency of 200 kHz and the switch-node voltage operating at 50% duty cycle, the proposed AEF is enabled and disabled, and the measured results are taken this time according to CISPR 25, an EMC standard for automotive, over a measurement range from 150 kHz to 3 MHz with a resolution bandwidth (RBW) of 9 kHz.

Shown in Fig. 7 is the conducted emissions result with DM noise measured separately. The DM attenuation at 200 kHz and 600 kHz with AEF enabled is 15 dB and 12 dB, respectively. Meanwhile, shown in Fig. 8 is the corresponding result for CM, where the additional CM attenuation at 200 kHz and 600 kHz with AEF enabled is 40 dB and 15 dB, respectively

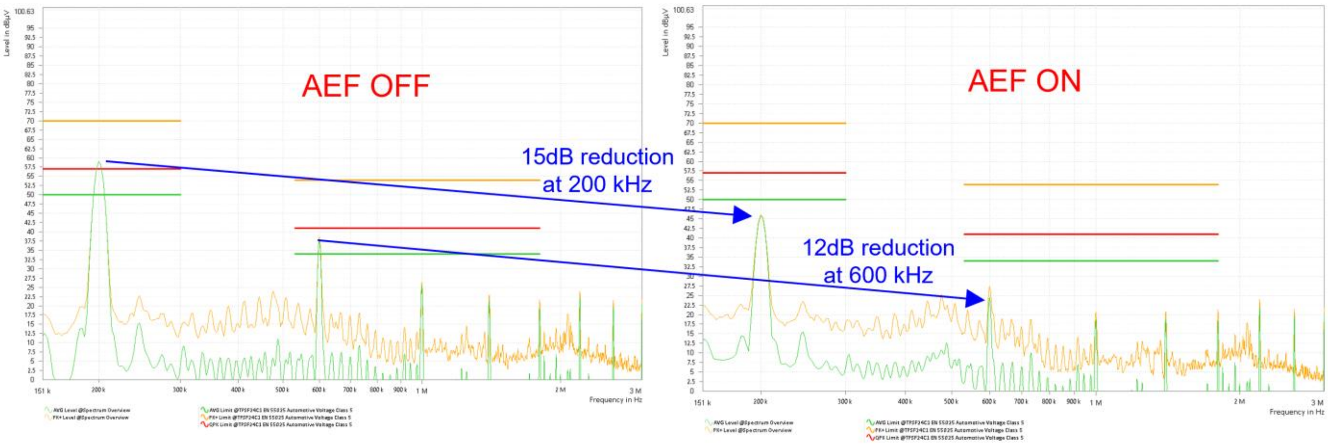

Fig. 7. CISPR 25 interference spectra for DM noise with the proposed AEF enabled/disabled for comparison.

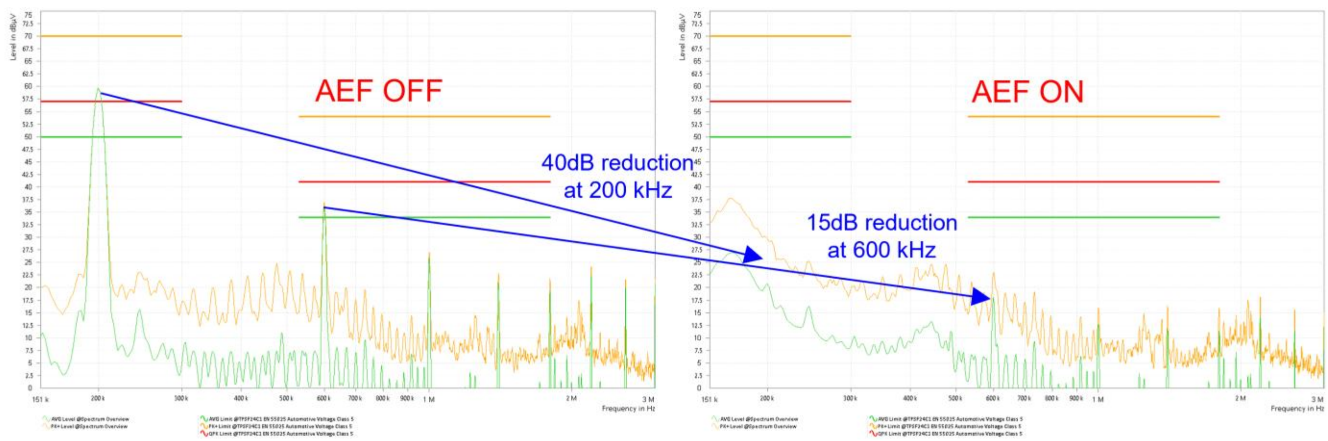

Fig. 8. CISPR 25 interference spectra for CM noise with the proposed AEF enabled/disabled for comparison.

Summary

Passive EMI filters generally occupy a significant amount of space, where especially the magnetic components—CM chokes and DM chokes—are the main cost and weight adders. To this end, AEF circuits receive significant attention for power electronics-constrained applications to improve the gravimetric (kW/kg), volumetric (kW/l) and cost (kW/$) density metrics of an EMI filter implementation.

The analysis in this article centers on a unified AEF circuit to attenuate the total noise, DM and CM, and thus reduce both the CM and DM choke inductances. A common bias supply referenced to chassis ground (not neutral) conveniently powers both AEF branches. The DM results obtained with the proposed architecture using an X-capacitor of 220 nF are similar to that of a passive solution with 2.2 μF installed at the C_{X2} schematic position (between the CM chokes).

An additional insertion loss of 15 dB to 20 dB for DM noise below 200 kHz is possible with the proposed circuit, hence allowing the use of smaller DM chokes or just relying on the leakage inductance of the CM choke, already made physically smaller with CM AEF.

References

1. "How Active EMI Filter ICs Reduce Common-Mode Emissions In Single- And Three-Phase Applications (Part 1): An Overview" by Timothy Hegarty, How2Power Today, November 2023 issue.

2. "How Active EMI Filter ICs Reduce Common-Mode Emissions In Single- And Three-Phase Applications (Part 2): Modeling Ferrite Chokes" by Timothy Hegarty, How2Power Today, February 2024 issue.

3. "How Active EMI Filter ICs Reduce Common-Mode Emissions In Single- And Three-Phase Applications (Part 3): Modeling Nanocrystalline Chokes" by Timothy Hegarty, How2Power Today, March 2024 issue.

4. "How Active EMI Filter ICs Reduce Common-Mode Emissions In Single- And Three-Phase Applications (Part 4): Loop-Gain Analysis" by Timothy Hegarty, How2Power Today, June 2024 issue.

5. "How Active EMI Filter ICs Reduce Common-Mode Emissions In Single- And Three-Phase Applications (Part 5): Improving Immunity To Low-Frequency Disturbances" by Timothy Hegarty, How2Power Today, May 2025 issue.

6. "Parameter Estimation of a Single-Phase Boost PFC Converter with EMI Filter Based on an Optimization Algorithm," by Gabriel Rojas-Dueñas, Jordi-Roger Riba and Manuel Moreno-Eguilaz, Electronics 10, no. 11: 1231, May 2021.

7. "Electromagnetic compatibility of multimedia equipment – Emission requirements," International Electrotechnical Commission, CISPR 32, second edition, March 2015.

8. "Implementation of an Active Common Mode EMI Filter Considering High Conducted Differential Mode EMI in Electric Vehicle On-Board Chargers" by Patrick Körner et al., 2024 Energy Conversion Congress and Expo (ECCE Europe), Germany, September 2024, pp. 1-7.

9. "A Novel Active EMI Filter Based on Transferring Common-Mode Noise to Differential-Mode Noise" by Hongpeng Wang et al., IEEE Transactions on Power Electronics, vol. 40, no. 7, pp. 8950-8955, July 2025.

10. "A New Integrated Active EMI Filter Topology With Both CM Noise and DM Noise Attenuation," by Yongxing Zhou et al., IEEE Transactions on Power Electronics, vol. 37, no. 5, pp. 5466-5478, May 2022.

11. "An Integrated Active EMI Filter to Attenuate Both DM and CM Noise in Single-Phase AC Systems" by Timothy Hegarty and Naresh Adepu, PCIM Europe 2026; Nuremberg, Germany, June 2026.

12. "Methods of measurement of touch current and protective conductor current," International Electrotechnical Commission, IEC 60990, third edition, May 2016.

13. "Characterization and Circuit Modeling of Electromagnetic Interference Filtering Chokes in Power Electronics: A Review" by Huamin Jie et al., IEEE Transactions on Power Electronics, vol. 40, no. 1, pp. 920-943, Jan. 2025.

About The Author

Timothy Hegarty is a senior member technical staff in the Switching Regulators business unit at Texas Instruments. With over 25 years of power-management engineering experience, he has written numerous conference papers, technical articles, seminars, white papers and application notes. Tim's current focus is on enabling technologies for high-frequency, low-EMI, switching regulators with a wide input-voltage range, targeting automotive, industrial, and datacenter applications. He is a senior member of the IEEE and a member of the IEEE Power Electronics Society.

For more on EMI and electromagnetic compatibility topics in power-supply design, see How2Power's Power Supply EMI Anthology.

